JOURNAL OF Applied Polymer SCIENCE

Hydrolytic degradation and crystallization behavior of linear 2-armed and star-shaped 4-armed poly(L-lactide)s: Effects of branching architecture and crystallinity

Hideto Tsuji, Toshiki Hayashi
Department of Environmental and Life Sciences, Graduate School of Engineering, Toyohashi University of Technology, Tempaku-cho, Toyohashi Aichi 441-8580, Japan
Correspondence to: H. Tsuji (E-mail: tsuji@ens.tut.ac.jp)

ABSTRACT: "Linear" aliphatic polyesters composed of two poly(L-lactide) arms attached to 1,3-propanediol and "star-shaped" ones composed of four poly(L-lactide) arms attached to pentaerythritol (2-L and 4-L polymers, respectively) with number-average molecular weight (M_n) = 1.4–8.4 × 10^4g/mol were hydrolytically degraded at 37°C and pH = 7.4. The effects of the branching architecture and crystallinity on the hydrolytic degradation and crystalline morphology change were investigated. The degradation mechanism of initially amorphous and crystallized 2-L polymers changed from bulk degradation to surface degradation with decreasing initial M_n; in contrast, initially crystallized higher molecular weight 4-L polymer degraded via bulk degradation, while the degradation mechanism of other 4-L polymers could not be determined. The hydrolytic-degradation rates monitored by molecular-weight decreases decreased significantly with increasing branch architecture and/or higher number of hydroxyl groups per unit mass. The hydrolytic degradation rate determined from the molecular weight decrease was higher for initially crystallized samples than for initially amorphous samples; however, that of 2-L polymers monitored by weight loss was larger for initially amorphous samples than for initially crystallized samples. Initially amorphous 2-L polymers with an M_n below 3.5 × 10^4g/mol crystallized during hydrolytic degradation. In contrast, the branching architecture disturbed crystallization of initially amorphous 4-L polymers during hydrolytic degradation. All initially crystallized 2-L and 4-L polymers had δ-form crystallites before hydrolytic degradation, which did not change during hydrolytic degradation. During hydrolytic degradation, the glass transition temperatures of initially amorphous and crystallized 2-L and 4-L polymers and the cold crystallization temperatures of initially amorphous 2-L and 4-L polymers showed similar changes to those reported for 1-armed poly(L-lactide). © 2015 Wiley Periodicals, Inc. J. Appl. Polym. Sci. **2015**, *132*, 41983.

KEYWORDS: biodegradable; biomaterials; biopolymers and renewable polymers; crystallization; degradation

Received 29 July 2014; accepted 8 January 2015
DOI: 10.1002/app.41983

INTRODUCTION

Poly(lactide)s [i.e., poly(lactic acid)s (PLAs)] are utilized for biomedical, pharmaceutical, and environmental applications.[1–11] The degradation mechanism, behavior, and rate of PLA-based materials depend on their molecular structures, higher order structures, fillers or additives, and material morphology. The degradation rate of PLA-based materials should be tuned depending on the application and purpose. Among the available molecular structures, the effects of the molecular weight and type, fraction, and distribution of comonomer units have been intensively studied to control the degradation rate and behavior of PLA-based materials.[12,13] The multifunctional alcohols that are incorporated during ring-opening polymerization of lactides (i.e., the cyclic dimer of lactic acid) induce the formation of linear and star-shaped (branching) architectures, increased numbers of hydroxyl-terminal groups per unit mass, and a change in the chain direction in the middle of the molecules for PLAs with 2 or more arms. In contrast, PLAs with linear architectures (i.e., 1-armed PLAs) and the coinitiator moieties incorporated at the end of molecules do not undergo a change in chain direction in the middle of the molecules.[14–16]

Yuan *et al.*, hydrolytically degraded linear 1-armed poly(DL-lactide) [i.e., poly(DL-lactic acid) (PDLLA)] and star-shaped 6-armed PDLLA with similar molecular weights and found that the hydrolytic-degradation rate, as monitored by weight loss, was higher for the 6-armed PDLLA.[17] Fu *et al.* hydrolytically degraded 1-armed PDLLA and multi-armed PDLLA synthesized with epoxidized soybean oil and reported that multiarmed

Additional Supporting Information may be found in the online version of this article.

© 2015 Wiley Periodicals, Inc.

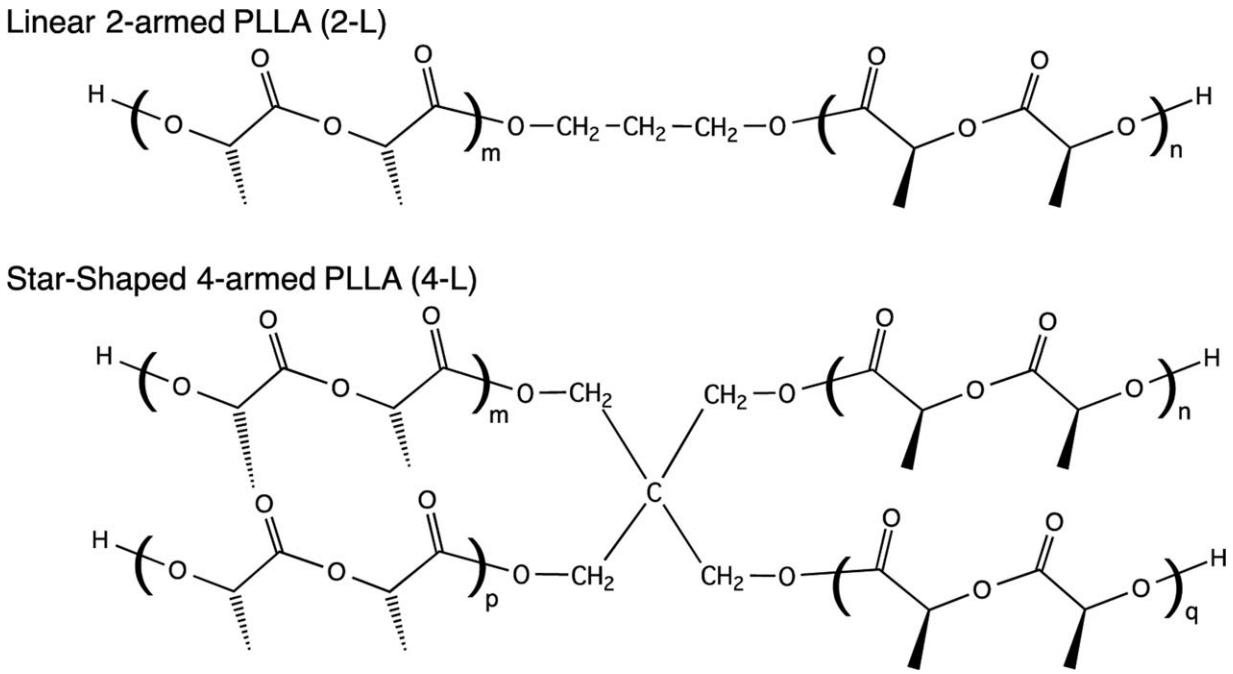

Figure 1. Molecular structures of linear 2-armed PLLA (2-L) and star-shaped 4-armed PLLA (4-L).

PDLLA had a lower hydrolytic degradation rate, as traced by weight loss and molecular weight decrease, than 1-armed PDLLA.[18] However, in these cases, the effects of the presence or absence of chain-directional change in the middle of the molecules and differences in the types of terminal groups (i.e., one carboxyl and one hydroxyl group for 1-armed PDLLA and four and six hydroxyl groups for 4- and 6-armed PDLLA, respectively) on hydrolytic degradation were not excluded. In a previous study, the relative hydrolytic degradation of 1-armed (carboxyl- and hydroxyl-terminated) and 2-armed (hydroxyl-terminated) amorphous PDLLAs was investigated in a phosphate-buffered solution at 97°C to determine the isolated effects of the chain directional change and coinitiator moiety in the middle of molecules and types of terminal groups.[15] Moreover, a comparative hydrolytic degradation study of 2-armed (hydroxyl-terminated) and 4-armed (hydroxyl-terminated) amorphous PDLLA was performed in phosphate-buffered solution at 97°C to elucidate the effects of star-shaped (branching) architectures and/or the number of terminal hydroxyl groups per unit mass on hydrolytic degradation.[16] The degradation mechanism gradually changes from bulk degradation to surface degradation with increasing number of arms and hydroxyl groups per unit mass.[15,16] Surprisingly, no significant change in molecular weight was observed for 4-armed PDLLA even when the samples were exposed to aqueous media at 97°C.[16] However, the hydrolytic degradation in these studies was carried out at the elevated temperature of 97°C for a short period of only 10 h. The information obtained during such accelerated hydrolytic degradation is likely different from that occurs at body temperature (37°C) over a long time period, as was performed in our previous study on linear 1-armed poly(L-lactide) [i.e., poly(L-lactic acid) (PLLA)], which was 3 year study.[19] Information obtained from hydrolytic degradation at body temperature is crucial for biomedical and pharmaceutical applications. Furthermore, Anderson *et al.* investigated the hydrolytic degradation of PLLA stereocomplexed with star-shaped poly(D-lactide) [i.e., poly(D-lactic acid) (PDLA)] oligomers with different numbers of arms and found that the stereocomplex crystallinity, number of arms and end-groups of the star-shaped PDLA oligomers clearly altered the degradation rate and affected the degradation-product patterns.[20]

The crystallization behavior of crystallizable 1-, 2-, and 4-armed poly(L-lactide) [i.e., poly(L-lactic acid) (PLLA)] from the melt was also investigated.[14,21] It was found that the branching architecture and chain-directional change and coinitiator moiety in the middle of the molecules and/or an increased number of terminal hydroxyl groups and decreased number of carboxyl groups per unit mass decelerated crystallization; however, these factors did not affect the glass transition temperature (T_g) or melting temperature (T_m) of molecules with similar number-average molecular weight (M_n) values or M_n values per arm. Kim *et al.* investigated the hydrolytic degradation of linear 1-armed and star-shaped 4-armed PLLAs and found that the molecular weight decrease was initially faster for 1-armed PLLA than for 4-armed PLLA but this trend reversed at a later stage.[22] In this case, however, the effects of chain-directional change and the coinitiator moiety in the middle of the molecules, differences in types of terminal groups, and the crystallinity of PLLAs were not excluded, and the crystallization behavior during hydrolytic degradation of 1-armed and 4-armed PLLAs was not reported.

To the best of our knowledge, the isolated effects of branching architecture (and/or increased number of terminal hydroxyl groups per unit mass) and crystallinity on hydrolytic degradation and the crystallization behavior of linear 2-armed and star-shaped 4-armed PLLAs (hereafter abbreviated as 2-L and 4-L polymers, respectively, Figure 1) during hydrolytic degradation have not yet been reported. In the present study, to investigate the isolated effects of the branching architecture (and/or

Table I. Molecular Characteristics of Linear 2-Armed and Branched 4-Armed PLLAs (2 and 4-L Polymers, Respectively) After Purification and Before Thermal Treatment

Arm number	Coinitiator	Code	LLA/coinitiator[a] (mol/mol)	M_n (GPC)[b] (g mol^{-1})	M_n (GPC) per one arm[b] (g mol^{-1})	M_n (NMR)[c] (g mol^{-1})	M_w(GPC)[b]/M_n(GPC)
2	1,3-Propanediol	2-L14	69/1	1.42×10^4	7.10×10^3	8.55×10^3	1.13
		2-L36	208/1	3.59×10^4	1.80×10^4	2.04×10^4	1.32
		2-L56	417/1	5.62×10^4	2.81×10^4	3.10×10^4	1.52
4	Pentaerythritol	4-L48	208/1	4.79×10^4	1.20×10^4	2.90×10^4	1.25
		4-L84	417/1	8.43×10^4	2.11×10^4	4.67×10^4	1.10

[a] L-Lactide (LLA)/coinitiator ratio for polymer synthesis.
[b] M_w (GPC) and M_n (GPC) are the weight- and number-average molecular weights, respectively, as evaluated by GPC.
[c] M_n (NMR) was calculated from M_n (GPC) using eqs. (1) and (2) for 2 and 4-L, respectively.

increased number of terminal hydroxyl groups per unit mass) and crystallinity on the hydrolytic-degradation and crystallization behavior of PLLAs, linear 2-L and star-shaped 4-L polymers with M_n values in the range of 1.4–8.4 $\times$ 10^4 g mol^{-1} were synthesized; their hydrolytic degradation and crystallization behavior were investigated at 37°C using initially amorphous and crystallized samples. The relatively low degradation temperature of 37°C (i.e., body temperature) in the present study as compared to the high degradation temperature of 97°C in the previous studies[15,16] was selected to avoid rapid crystallization of 2-L and 4-L polymers at temperatures above the T_g (i.e., 50–60°C), which would reduce the crystallinity differences between the initially amorphous and crystallized samples, and to accumulate information beneficial to biomedical and pharmaceutical applications.

EXPERIMENTAL

Materials

Linear 2-L and star-shaped 4-L polymers were synthesized by ring-opening polymerization of L-lactide (PURASORB L®, Purac Biomaterials, Gorinchem, The Netherlands) in bulk at 140°C for 10 h initiated using 0.03 wt % tin(II) 2-ethylhexanoate (Nacalai Tesque, Kyoto, Japan) in the presence of varying amounts of 1,3-propanediol (Sigma-Aldrich, St. Louis, MO) and pentaerythritol (Sigma-Aldrich) as the coinitiators.[21,23] Before polymerization, L-lactide was purified by repeated recrystallization from ethyl acetate (guaranteed grade, Nacalai Tesque). Tin(II) 2-ethylhexanoate was purified by distillation under reduced pressure. 1,3-Propanediol and pentaerythritol were used as received. By altering the ratios of the coinitiator to L-lactide, 2-L and 4-L polymers with different M_n values were synthesized. The synthesized polymers were purified by dissolution in chloroform (guaranteed grade, Nacalai Tesque) followed by reprecipitation using methanol (guaranteed grade, Nacalai Tesque). The purified polymers were dried under reduced pressure for at least seven days. The molecular characteristics and thermal properties of 2-L and 4-L polymers used in this study are listed in Table I. Here, the numbers immediately following the terms of 2-L and 4-L polymers show the M_n values in units of 10^3 g mol^{-1} and 'A' and 'C' immediately following the M_n values indicate that the compounds were amorphous and crystallized, respectively, before hydrolytic degradation. Schwach and Vert reported that the hydrophobic tin(II) 2-ethylhexanoate residue in PLLA delays water uptake and hydrolytic degradation.[24] However, in the present study, we synthesized 2-L and 4-L polymers at the same low concentration of tin(II) 2-ethylhexanoate of 0.03 wt % and the did not find evidence of 2-ethylhexanoate residue via ^{1}H NMR spectroscopy. Therefore, 2-ethylhexanoate residue will not affect the water uptake and hydrolytic degradation of the polymers.

The solution-cast samples, which were ~100 μm thick, were prepared at 25°C using dichloromethane as the solvent. After solvent evaporation under atmospheric pressure, the cast samples were further dried under reduced pressure for at least seven days before being subjected to thermal treatment. To prepare the amorphous samples, each sample was sealed in a test tube under reduced pressure, melted at 200°C for 5 min, and then quenched at 0°C for 5 min. To prepare the crystallized samples, the amorphous samples were crystallized at 120°C for 10 min. The crystallization time was short compared to that for direct crystallization from the melt because the quenching process before crystallization induced the formation of a high number of spherulite nuclei per unit mass, resulting in rapid crystallization.[25]

Hydrolytic Degradation

Hydrolytic degradation of each sample (~100 μm thick, ~25 mg) was performed in 10 mL of phosphate-buffered solution (pH 7.4) at 37°C; one sample was used for each experimental point. After hydrolytic degradation, the samples were rinsed twice with fresh distilled water (HPLC grade, Nacalai Tesque), soaked in fresh distilled water for one day, and then dried under reduced pressure for at least seven days.

Measurements

The weight-average molecular weight (M_w) and M_n values of the samples were evaluated in chloroform at 40°C using a Tosoh (Tokyo, Japan) GPC system with two TSK gel columns (GMH_{XL}, Tosoh) and polystyrene standards. Calibration was performed in the molecular weight range of 5.00 $\times$ 10^3−8.42 $\times$ 10^6 g mol^{-1}. The M_w and M_n values estimated by GPC are referred to as M_w (GPC) and M_n (GPC), respectively. From a previous study, the M_n (GPC) values of the 2-L and 4-L polymers were correlated to the M_n values estimated by ^{1}H NMR

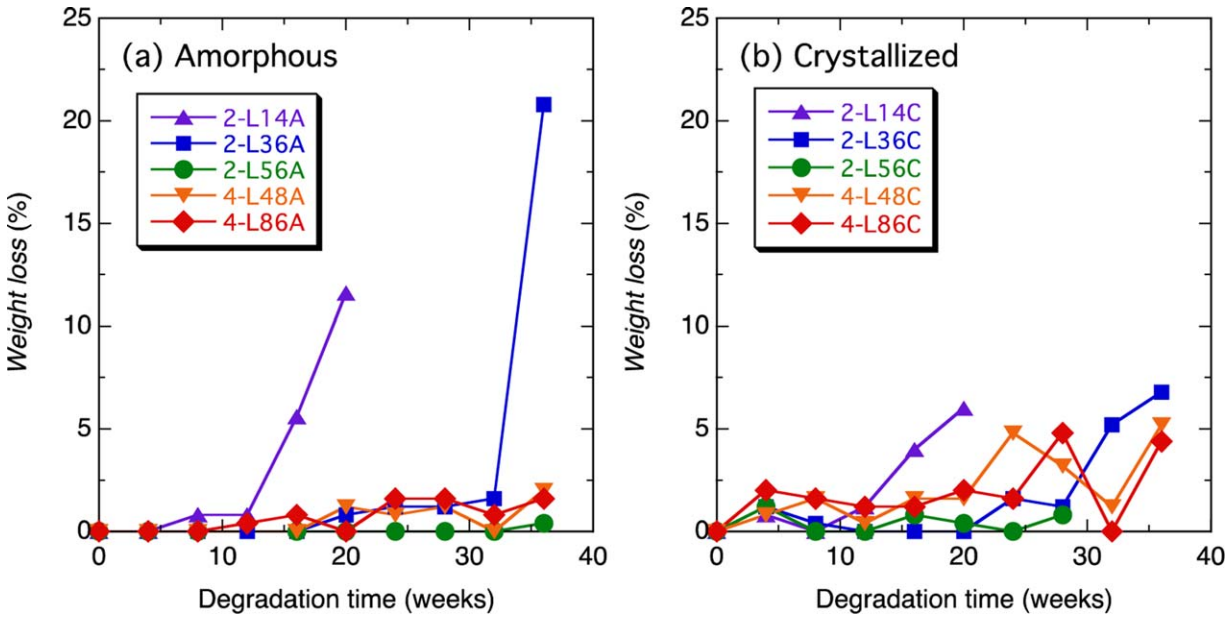

Figure 2. Weight losses of initially amorphous (a) and crystallized (b) 2-L and 4-L samples during hydrolytic degradation as a function of degradation time. [Color figure can be viewed in the online issue, which is available at wileyonlinelibrary.com.]

spectroscopy [M_n(NMR)] to eliminate the effects of molecular architecture,[21,23] as shown in the following equations:

$$M_n(\text{NMR}) = 1.10 \times M_n(\text{GPC})^{0.937} (\text{2-L polymers}) \quad (1)$$

$$M_n(\text{NMR}) = 3.40 \times M_n(\text{GPC})^{0.840} (\text{4-L polymers}) \quad (2)$$

Using eqs. (1) and (2), the M_n(GPC) values were converted to M_n(NMR) values. The crystallinity (X_c) values of the samples were estimated using wide-angle X-ray diffractometry (WAXD). The WAXD measurements were performed at 25°C using a Rigaku (Tokyo, Japan) RINT-2500 equipped with a Cu-K_α source (λ = 0.15418 nm), which was operated at 40 kV and 200 mA. In the 2θ range of 7.5°–25.0°, the crystalline diffraction peak area relative to the total area between the diffraction profile and baseline was used to determine the X_c values. The glass transition, cold crystallization, and melting temperatures (T_g, T_{cc}, and T_m, respectively) and enthalpies of cold crystallization and melting (ΔH_{cc} and ΔH_m, respectively) of the samples were determined using a Shimadzu (Kyoto, Japan) DSC-50 differential scanning calorimeter under a nitrogen gas flow rate of 50 mL min^{-1}. The samples (~3 mg) were heated from room temperature to 200°C at a rate of 10°C min^{-1}. The T_g, T_{cc}, and T_m values were calibrated using tin, indium, and benzophenone (all guaranteed grade, Nacalai Tesque) as standards. The weight losses of the samples after hydrolytic degradation were determined using the following equation:

$$\text{Weight loss (\%)} = 100 \times (W_b - W_a)/W_b \quad (3)$$

where W_b and W_a are the sample weights before and after hydrolytic degradation, respectively.

Data Analysis

One-way analysis of variance (ANOVA) was performed on the M_n (GPC) values of the hydrolytically degraded samples to determine the significance at 95% confidence. The samples were divided into two groups for the former and latter half of each degradation period to judge the significance of the M_n (GPC) decrease during immersion in a phosphate-buffered solution.

RESULTS AND DISCUSSION

Weight Loss

Weight loss during hydrolytic degradation is caused by the formation of water-soluble low molecular weight oligomers and monomers formed by chain cleavage and their release from the materials. Therefore, weight loss can be used as an indicator of the fraction of water-soluble low molecular weight oligomers and monomers formed within the materials.[15,16] During bulk degradation, the degradation process can be divided into two stages: In the first stage, a significant molecular weight decrease with no significant weight loss occurs; in the second stage, a significant weight loss takes place in addition to a molecular weight decrease. During surface degradation, a significant weight loss occurs with no significant molecular weight decrease.

Figure 2 shows the weight losses of hydrolytically degraded amorphous and crystallized 2-L and 4-L samples. The weight losses at 20 weeks are plotted in Figure 3(a,d) as functions of the initial M_n(GPC) and M_n(GPC) values per arm, respectively. Considering the distribution of data, a significant weight loss (>5%) was only observed for the following 2-L samples: Initially amorphous 2-L14A (16 weeks) and 2-L36A (36 weeks) and initially crystallized 2-L14C (20 weeks) and 2-L36C (36 weeks). The induction period difference of 2-L samples can be explained by the difference in the molecular weights; that is, a shorter induction period was required for the formation of water-soluble low–molecular–weight oligomers in the sample with a lower molecular weight. Comparison of the initially amorphous and crystallized samples of 2-L14 and 2-L36 revealed that the weight loss values were higher for the amorphous samples. In the case of 2-L samples, the induction period

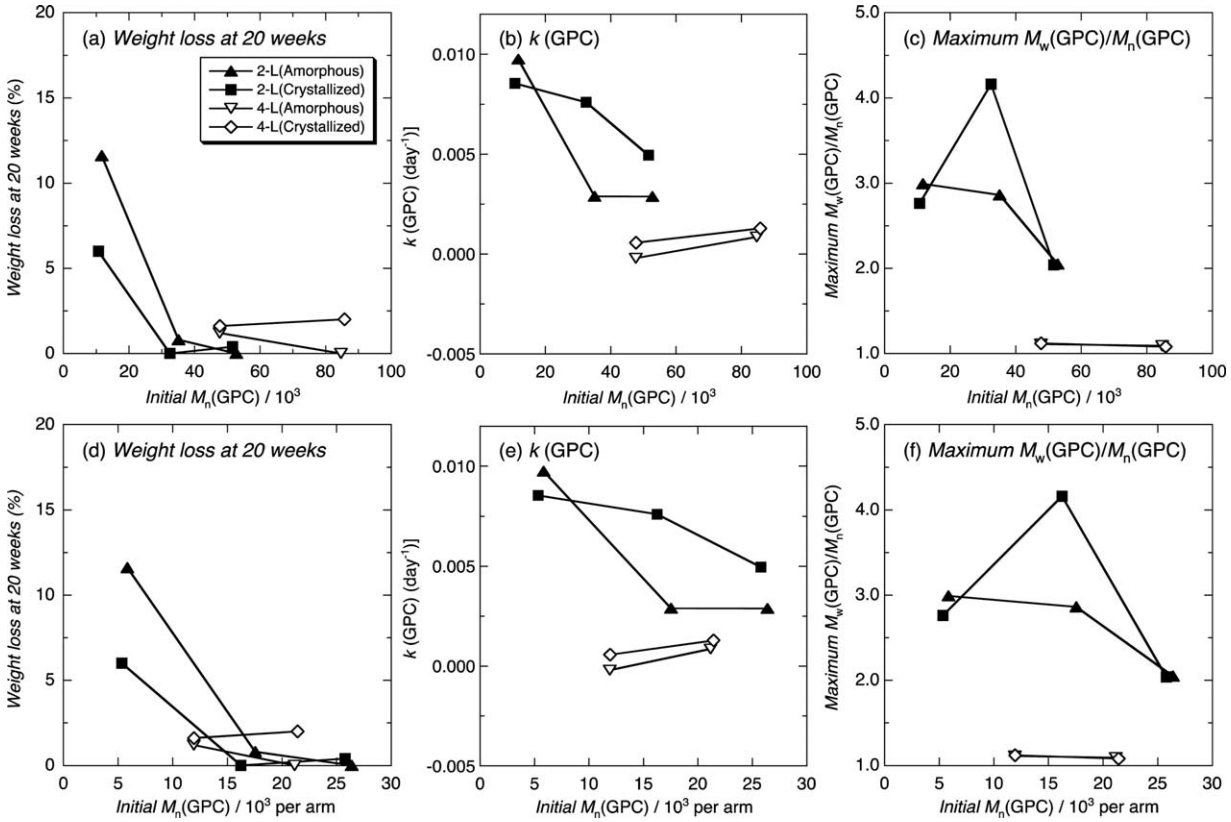

Figure 3. Weight losses at 20 weeks (a, d), hydrolytic degradation rate constants [k(GPC)] (b, e), maximum M_w/M_n (c,f) as functions of initial M_n(GPC)/10^3 (a–c) and M_n(GPC)/10^3 per arm (d–f).

for significant weight loss and the weight loss at 20 weeks respectively increased and decreased with increasing initial M_n(GPC) or M_n(GPC) value per arm. Because there were no significant differences in the weight losses of 2-L and 4-L at 20 weeks, the effects of the molecular architecture (and/or number of terminal hydroxyl groups per unit mass) could not be determined. Furthermore, for the 4-L samples, the effects of crystallinity could not be assessed because of their low weight loss values.

Molecular Weight

To elucidate the molecular-level degradation, GPC measurements were performed. Figures S1 and S2, Supporting Information show GPC profiles of initially amorphous and crystallized 2-L and 4-L samples that were hydrolytically degraded for different periods of time. According to the results of one-way ANOVA analysis, the M_n(GPC) decreases were significant for all the samples except 4-L48A and 4-L48C. The GPC profiles of initially amorphous 2-L56A, initially crystallized 2-L56C, and 4-L84C all shifted toward lower molecular weights. This suggested that the hydrolytic degradation of these samples mainly proceeded via the bulk degradation mechanism. In contrast, either a high molecular weight fraction or all fractions remained unchanged or slightly increased in the GPC profiles of initially amorphous 2-L14A, 2-L36A, 4-L48A, and 4-L84A and initially crystallized 2-L14C and 4-L48C, which suggested that either the surface degradation mechanism was active or insignificant degradation of these samples occurred. 2-L36C underwent surface degradation during the first 20 weeks and bulk degradation subsequently. These results revealed that the degradation mechanism of initially amorphous and crystallized 2-L samples changed from bulk degradation to surface degradation with decreasing initial molecular weight; in contrast, the degradation mechanism of initially crystallized higher molecular weight 4-L (4-L84C) was bulk degradation while that of other 4-L samples could not be determined due to the insignificant molecular-weight decrease.

The M_n (GPC) values of 2-L and 4-L samples obtained from the GPC profiles in Figures S1 and S2, Supporting Information are plotted in Figure 4 as a function of degradation time. The M_n(NMR) values of 2-L and 4-L samples obtained from the M_n(GPC) values via eqs. (1) and (2) are shown in Figure S3, Supporting Information. The similarity between (a) and (b) in Figures 4 and S3, Supporting Information indicated that the crystallinity had a very small impact on the decrease of the M_n(GPC) or M_n(NMR) values. Monotonous decreases in M_n(GPC) and M_n(NMR) were observed for initially amorphous and crystallized 2-L samples. In contrast, either a very small decrease or no decrease in M_n(GPC) and M_n(NMR) was noted for initially amorphous and crystallized 4-L samples. Such insignificant changes in the M_n(GPC) and M_n(NMR) values of initially amorphous 4-L48A and 4-L48C were attributed to the removal of water-soluble components from the sample, which was evident from the disappearance of the bottom edge of the GPC profiles at the lower molecular-weight side at longer degradation periods. The hydrolytic degradation rate (k) values were

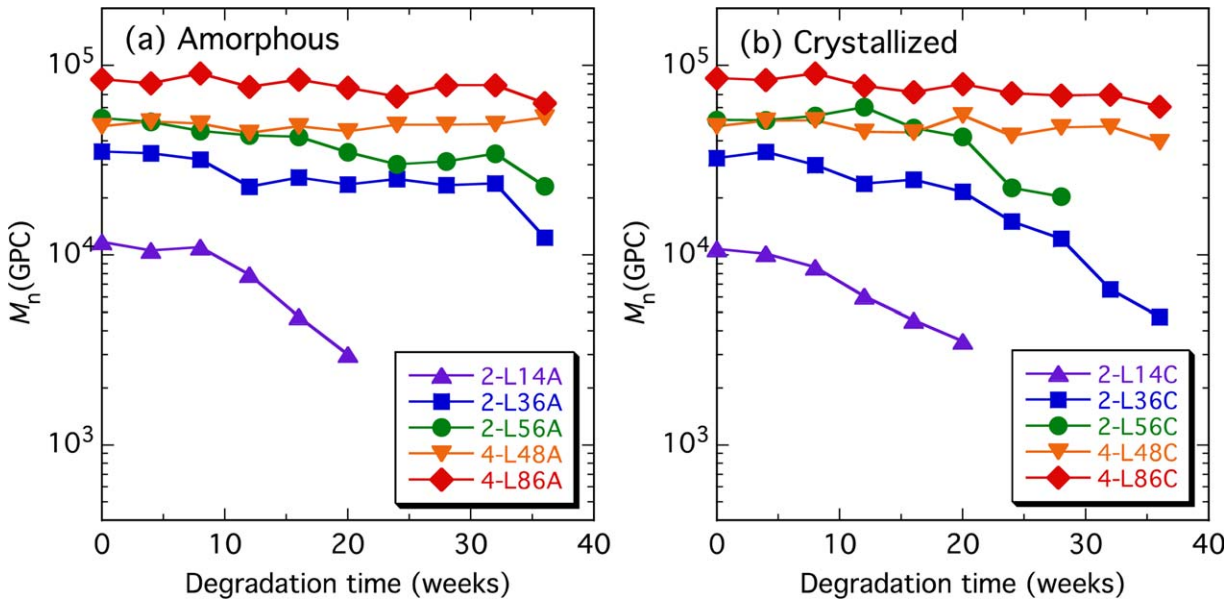

Figure 4. M_n(GPC) of initially amorphous (a) and crystallized (b) 2-L and 4-L samples during hydrolytic degradation as a function of degradation time. [Color figure can be viewed in the online issue, which is available at wileyonlinelibrary.com.]

estimated from Figure 4 according to the following equation[12,13]:

$$\ln M_n(t) = \ln M_n(t_0) - k(t - t_0) \quad (4)$$

where $M_n(t)$ and $M_n(t_0)$ are the M_n values at hydrolytic degradation times t and t_0, respectively. The k values obtained using M_n(GPC) and M_n(NMR) [k(GPC) and k(NMR), respectively] are summarized in Table II, and the k(GPC) values are plotted in Figures 3(b,e) as functions of the initial M_n(GPC) and M_n(GPC) values per arm, respectively. As seen in Table II, the k(NMR) values showed a dependence on M_n(GPC) and M_n(GPC) per arm similar to that of the k(GPC) values. The negative values of k(GPC) and k(NMR) for 4-L48A and 4-L48C indicated that the molecular weight increased because of insignificant degradation of the samples and removal of low molecular-weight water-soluble oligomers from the samples. The k(GPC) values of amorphous and crystallized 2-L samples were higher than those of amorphous and crystallized 4-L samples when compared at similar initial M_n(GPC) values or M_n(GPC) values per arm [Figures 3(b,e)]. The k(GPC) values of 2-L samples decreased with increasing initial M_n(GPC) and M_n(GPC) values per arm, whereas those of 4-L samples were almost constant around zero. The higher k(GPC) for the initially low molecular weight of 2-L samples was explained by the increased chain mobility and hydrophilic terminal groups per unit mass, which increased the diffusion rate and concentration of water in the sample.

The results here indicated that the branching architecture and/or the increased number of terminal hydroxyl groups per unit mass reduced the hydrolytic-degradation rate monitored by k(GPC). A similar result was observed for the hydrolytic degradation of 2- and 4-armed amorphous PDLLAs.[16] As stated in a previous study,[16] the higher number of terminal hydroxyl groups per unit mass that occurred with greater numbers of arms was postulated to accelerate hydrolytic degradation because the higher hydrophilicity of the hydroxyl groups attracted more water molecules; additionally, the higher number of terminal hydroxyl groups, around which cleavage of the ester groups occurred, elevated the cleavage rate[26] when the terminal hydroxyl groups were in the free state. However, the terminal hydroxyl groups could form hydrogen bonds with adjacent terminal hydroxyl groups; such intra- and intermolecular hydrogen bonding prevented the terminal hydroxyl groups from interacting with water molecules and participating in cleavage of the ester groups around the terminal hydroxyl groups resulting in hindered hydrolytic degradation. Furthermore, hydrogen bonding between different molecules increased the apparent molecular weight and thereby reduces the chain mobility. The decreased chain mobility would disturb the diffusion of water molecules into materials and delayed hydrolytic degradation.

For both 2-L and 4-L samples, the k(GPC) values were higher for the initially crystallized samples than for the initially amorphous samples, which was in agreement with the results reported for high molecular weight 1-armed linear PLLA[15,26]; thus, similar to the result for 1-armed PLLA, crystallization accelerated the hydrolytic degradation of linear 2-armed 2-L and star-shaped 4-armed 4-L.

M_w (GPC)/M_n (GPC) values were obtained from Figures S1 and S2, Supporting Information and are plotted in Figure 5 as a function of degradation time. The M_w(GPC)/M_n(GPC) values of 2-L samples increased with degradation time; the increase was remarkable for 2-L14A and 2-L14C in the period exceeding 8 weeks and for 2-L36A and 2-L36C in the periods exceeding 32 and 28 weeks, respectively. On the other hand, no significant increase was noticed for the 4-L samples. The maximum M_w(GPC)/M_n(GPC) values obtained from Figure 5 are plotted in Figure 3(c,f) as functions of the initial M_n(GPC) and M_n(GPC) values per arm, respectively. Regardless of the initial crystallinity and initial M_n(GPC) and M_n(GPC) values per arm,

Table II. Molecular Characteristics of Linear 2-Armed and Branched 4-Armed PLLAs (2 and 4-L Polymers, Respectively) Before and After Hydrolytic Degradation

Initial state[a]	Code	HDT[b] (weeks	M_n (GPC)[c] (g mol^{-1})	M_n (NMR)[d] (g mol^{-1})	M_w (GPC)[c] / M_n (GPC)	k (GPC)[e] (day^{-1})	k (NMR)[e] (g mol^{-1})
A	2-L14A	0	1.17×10^4	7.13×10^3	1.15	9.74×10^{-3}	9.13×10^{-3}
		20	2.99×10^3	1.99×10^3	2.99		
	2-L36A	0	3.51×10^4	2.00×10^4	1.23	2.88×10^{-3}	1.89×10^{-3}
		36	1.23×10^4	7.48×10^3	2.86		
	2-L56A	0	5.28×10^4	3.15×10^4	1.42	2.87×10^{-3}	2.69×10^{-3}
		36	2.30×10^4	1.57×10^4	2.05		
	4-L48A	0	4.77×10^4	2.89×10^4	1.15	-2.01×10^{-4}	-1.69×10^{-4}
		36	5.32×10^4	3.17×10^4	1.11		
	4-L84A	0	8.47×10^4	4.69×10^4	1.09	8.54×10^{-4}	7.18×10^{-4}
		36	6.33×10^4	3.67×10^4	1.09		
C	2-L14C	0	1.07×10^4	6.56×10^3	1.21	8.53×10^{-3}	7.99×10^{-3}
		20	3.51×10^3	2.31×10^3	2.76		
	2-L36C	0	3.25×10^4	1.86×10^4	1.33	7.59×10^{-3}	5.86×10^{-3}
		36	4.72×10^3	4.15×10^3	4.16		
	2-L56C	0	5.16×10^4	3.09×10^4	1.61	4.95×10^{-3}	4.15×10^{-3}
		28	2.03×10^4	1.41×10^4	2.04		
	4-L48C	0	4.78×10^4	2.90×10^4	1.15	5.63×10^{-4}	4.73×10^{-4}
		36	3.94×10^4	2.46×10^4	1.12		
	4-L84C	0	8.58×10^4	4.74×10^4	1.09	1.28×10^{-3}	1.07×10^{-3}
		36	6.06×10^4	3.54×10^4	1.08		

[a] A and C indicate amorphous and crystallized, respectively.
[b] Hydrolytic degradation time.
[c] M_w (GPC) and M_n (GPC) are the weight- and number-average molecular weights, respectively, as evaluated by GPC.
[d] M_n (NMR) was calculated from M_n (GPC) using eqs. (1) and (2) for 2-L and 4-L, polymers, respectively.
[e] k (GPC) and k(NMR) are the hydrolytic degradation constants estimated from M_n (GPC) and M_n (NMR), respectively.

the M_w(GPC)/M_n(GPC) values were much larger for 2-L samples than 4-L samples. The higher values of M_w(GPC)/M_n(GPC) for 2-L samples as compared with those for 4-L samples reflect the high degree of degradation and strongly suggested inhomogeneous degradation that depended on the depth from the material surface.

Higher-Order Structure

To investigate the higher-order structural changes during hydrolytic degradation, WAXD measurements were performed for the initially amorphous and crystallized samples after hydrolytic degradation for different periods of time (Figures S4 and S5, Supporting Information). Crystalline diffraction peaks at around 17° and 19° were observed for initially amorphous 2-L14A and 2-L36A after 20 and 24–36 weeks, respectively (Figure S4, Supporting Information) and all initially crystallized samples (Figure S5, Supporting Information) for which the peaks were assigned to (110)/(200) and (203) reflections of the α- or δ-form of PLLA crystallites.[27–31] The crystallinity (X_c) values were estimated from the WAXD profiles in Figures S4 and S5, Supporting Information and are plotted in Figure 6 as a function of hydrolytic degradation time. Initially amorphous 2-L56A and all 4-L samples remain amorphous during the hydrolytic degradation period studied here. In contrast, crystallization of PLLA segments occurred in initially amorphous 2-L14A and 2-L36A for degradation periods longer than 20 and 24 weeks, respectively. The results here were indicative of the fact that initially amorphous 2-L samples with an M_n(GPC) value of less than 3.5×10^4 g mol^{-1} was crystallizable during hydrolytic degradation, as in the case of 1-armed PLLA,[19,32–36] and that the branching architecture and/or higher density of terminal hydroxyl groups per unit mass disturbed the crystallization of initially amorphous 4-L samples during hydrolytic degradation. In addition to crystallization during hydrolytic degradation in the presence of water as a plasticizer, degradation and removal of the chains in the amorphous regions increased the X_c of 2-L14A and 2-L36A to maximum values of ~7 and 39%, respectively. For the initially crystallized samples, the X_c values remained unchanged during the degradation period studied here; this indicated that neither further crystallization nor selective degradation and removal of amorphous chains occurred in the crystallized samples during hydrolytic degradation. The selective removal of amorphous chains did not have a significant effect on the initially crystalline samples that had negligible or very low weight losses during hydrolytic degradation (Figure 2). However, longer hydrolytic degradation periods (>36 weeks) could potentially facilitate the crystallization of samples that did not crystallize within the periods studied here.

To elucidate the crystalline form (i.e., α- or δ-form) of the initially crystallized samples and the changes upon hydrolytic

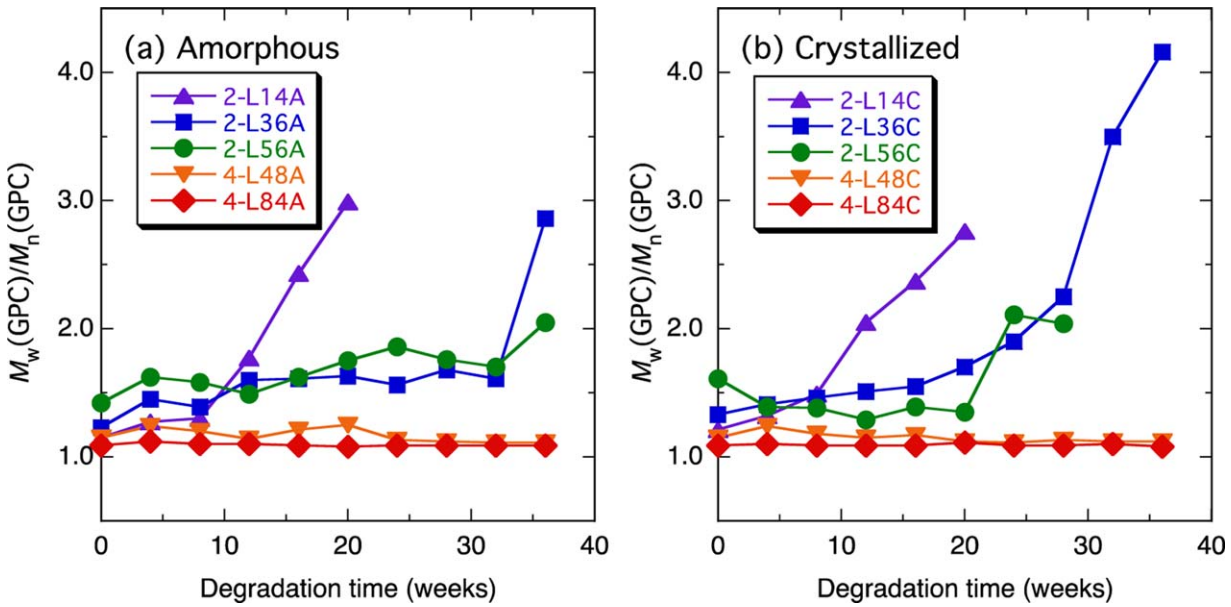

Figure 5. M_w(GPC)/M_n(GPC) of initially amorphous (a) and crystallized (b) 2-L and 4-L samples during hydrolytic degradation as a function of degradation time. [Color figure can be viewed in the online issue, which is available at wileyonlinelibrary.com.]

degradation, WAXD profiles of the samples before and after hydrolytic degradation for 36 weeks were magnified along the vertical direction (Figure 7). The crystalline diffraction angles of 12.5°, 22.5°, 24°, and 25°corresponded to the (004/103), (015), (016), and (206) reflections, respectively, of the α-form crystallites.[30] Of these peaks, the crystalline diffraction peaks at 24° and 25° were important for identifying the α- or δ-form. As seen, the set of crystalline diffraction peaks at 24° and 25°, which were characteristic of the α-form, were not observed for all initially crystallized samples before and after hydrolytic degradation. Instead, a single crystalline diffraction peak at 24.6°, which was characteristic of the δ-form,[30] was observed for all initially crystallized samples before and after hydrolytic degradation. These results indicated that all the initially crystallized samples included δ-form homo-crystallites as crystalline species and hydrolytic degradation did not alter the crystalline modification.

Thermal Properties

To elucidate the changes in the thermal properties during hydrolytic degradation, DSC measurements were performed. Figures S6 and S7, Supporting Information show the DSC thermograms of 2-L and 4-L samples, respectively, before and after hydrolytic degradation for different periods of time. In these figures, the glass transition, cold crystallization (only for the initially

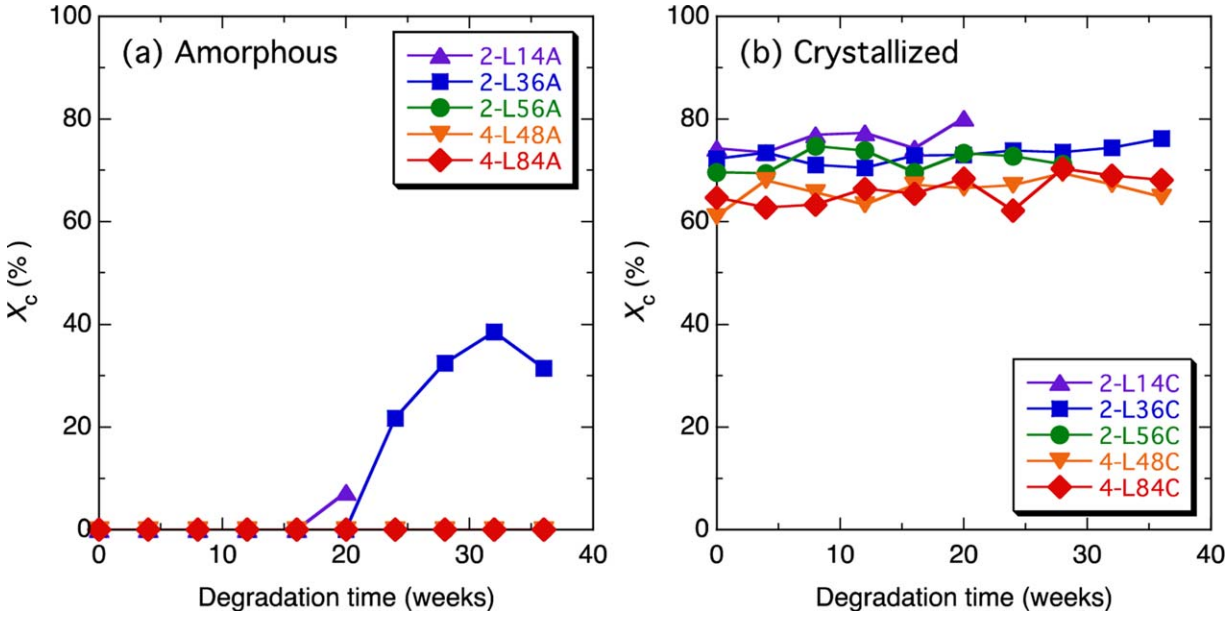

Figure 6. Crystallinity (X_c) of initially amorphous (a) and crystallized (b) 2-L and 4-L samples during hydrolytic degradation as a function of degradation time. [Color figure can be viewed in the online issue, which is available at wileyonlinelibrary.com.]

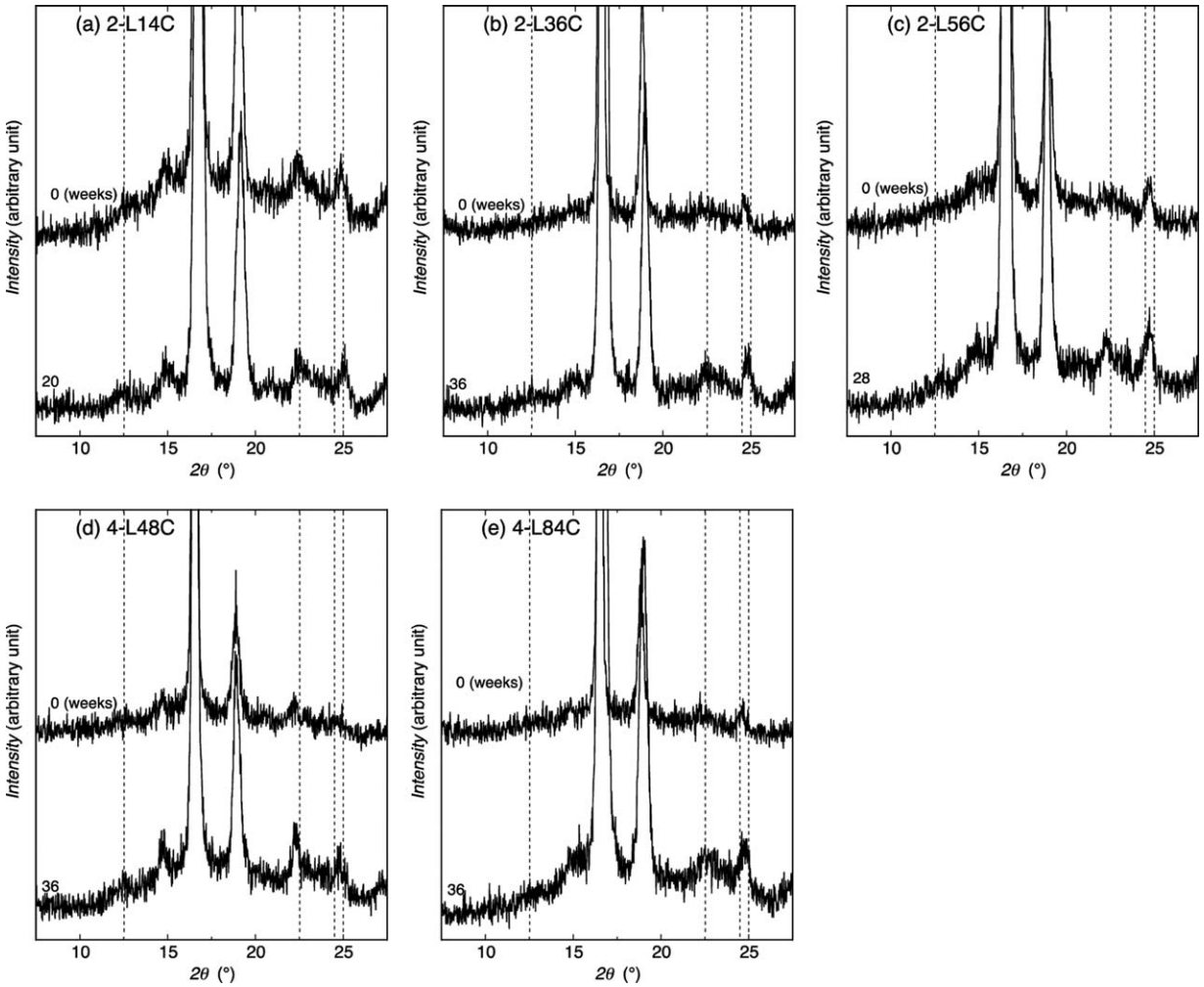

Figure 7. Magnified and smoothed WAXD profiles of initially crystallized 2-L and 4-L samples before and after hydrolytic degradation for 20, 28, or 36 weeks. Broken lines indicate the diffraction angles that are specific to the α-form.

amorphous samples), and melting peaks were observed at 50–70, 80–130, and 130–180°C, respectively. The thermal properties were estimated from the DSC thermograms in Figures S6 and S7, Supporting Information. The thermal properties thus obtained are tabulated in Table III and the T_g, T_{cc}, ΔH_{cc}, and T_m values of the lower temperature subpeak and higher temperature main peak are plotted in Figures 8–11 as a function of degradation time. In Figure 10, the T_m data are only provided for samples that had melting subpeaks at lower temperatures.

As seen in Figure 8, the T_g values of all the samples, except 2-L14A, increased by 5°C or more within 4–12 weeks and then decreased gradually with increasing degradation time. This trend has often been reported for 1-armed PLLA during hydrolytic degradation.[19,32,36] Normally, the initial increase was ascribed to the effect of low temperature annealing in the presence of water as a plasticizer, which stabilized chain packing and thereby reduced segmental mobility; in contrast, the later decrease was attributed to the decreased molecular weight, which resulted in increased segmental mobility. For the initially crystallized samples, the shortened chains with a free terminal group and the amorphous chains with a free terminal group formed from tie chains may have slightly reduced the M_n and have had a significant effect on elevating the segmental mobility of the amorphous chains. In contrast, for the initially amorphous samples, although 2-L36A and 2-L56A featured a gradually decreasing or constant T_g value after the initial increase of about 5°C at four weeks, the T_g of other initially amorphous samples showed complicated changes or distributions. The distribution was larger for 4-L samples than for 2-L samples; this may have been caused by the high density of hydrophilic terminal hydroxyl groups at lower molecular weights, which may have resulted in hydrogen bonding between the different molecules thereby reducing the chain mobility and increasing the T_g.

The T_{cc} values of all the samples, except for 2-L14A, rapidly decreased during the first four weeks and then slowly decreased or remained steady (Figure 9). The initial rapid decrease in T_{cc} was ascribed to the stabilized chain packing caused by low-temperature annealing in the presence of water, which facilitated nucleation and crystallization at a lower temperature; this is consistent with the results reported for 1-armed PLLA.[19,32] The later slow decrease in T_{cc} occurred because of the decreased molecular weight, which increased the segmental mobility and facilitated

Table III. Thermal Properties of Linear 2-Armed and Branched 4-Armed PLLAs (2 and 4-L Polymers, Respectively) Before and After Hydrolytic Degradation

Initial state[a]	Code	HDT[b] (weeks)	T_g[c] (°C)	T_{cc}[c](°C)	T_m[c](°C)	ΔH_{cc}[d](°C)	ΔH_m[d](J g^{-1})	$\Delta H_{cc} + \Delta H_m$[d] (J g^{-1})
A	2-L14A	0	53.6	95.3	152.3	−50.7	50.4	−0.3
		20	64.3	82.8	143.1	−31.4	40.7	9.3
	2-L36A	0	56.5	103.7	166.0	−50.7	50.4	−0.3
		36	55.6	87.1	165.1	−49.1	49.6	0.5
	2-L56A	0	56.3	110.5	172.8	−50.7	51.5	0.8
		36	59.8	90.7	161.3, 169.8	−49.2	50.3	1.1
	4-L48A	0	57.3	126.1	163.1	−41.5	41.9	0.4
		36	58.4	96.0	150.8, 162.2	−41.4	42.9	1.5
	4-L84A	0	56.7	106.8	156.3, 167.8	−43.0	43.8	0.8
		36	58.2	91.6	155.6, 166.4	−46.0	45.6	−0.4
C	2-L14C	0	49.6		152.4		50.2	50.2
		20	–[e]		149.9		57.3	57.3
	2-L36C	0	–[e]		165.3		57.8	57.8
		36	–[e]		163.1		52.6	52.6
	2-L56C	0	57.4		161.3, 171.3		49.9	49.9
		28	–[e]		169.9		49.0	49.0
	4-L48C	0	57.7		154.8, 162.7		48.2	48.2
		36	–[e]		162.9		51.5	51.5
	4-L84C	0	59.9		154.7, 167.6		43.4	43.4
		36	–[e]		163.9		56.8	56.8

[a] A and C indicate amorphous and crystallized, respectively.
[b] Hydrolytic degradation time.
[c] T_g, T_{cc}, and T_m are the glass transition, cold crystallization, melting temperatures, respectively.
[d] ΔH_{cc} and ΔH_m are the enthalpies of cold crystallization and melting, respectively.
[e] The glass transition peak was too diffuse to estimate T_g.

nucleation and crystallization at a lower temperature. The T_{cc} of 2-L14A split into higher and lower values after 4 weeks, returned to a single value after 8 weeks, and then decreased T_{cc} at 20 weeks. The T_{cc} values of 4-L48A and 4-L84A decreased rapidly for the first 4 weeks, decreased slowly for the period of 4–20 and 4–16 weeks, and split into higher and lower values at 24 and 20 weeks,

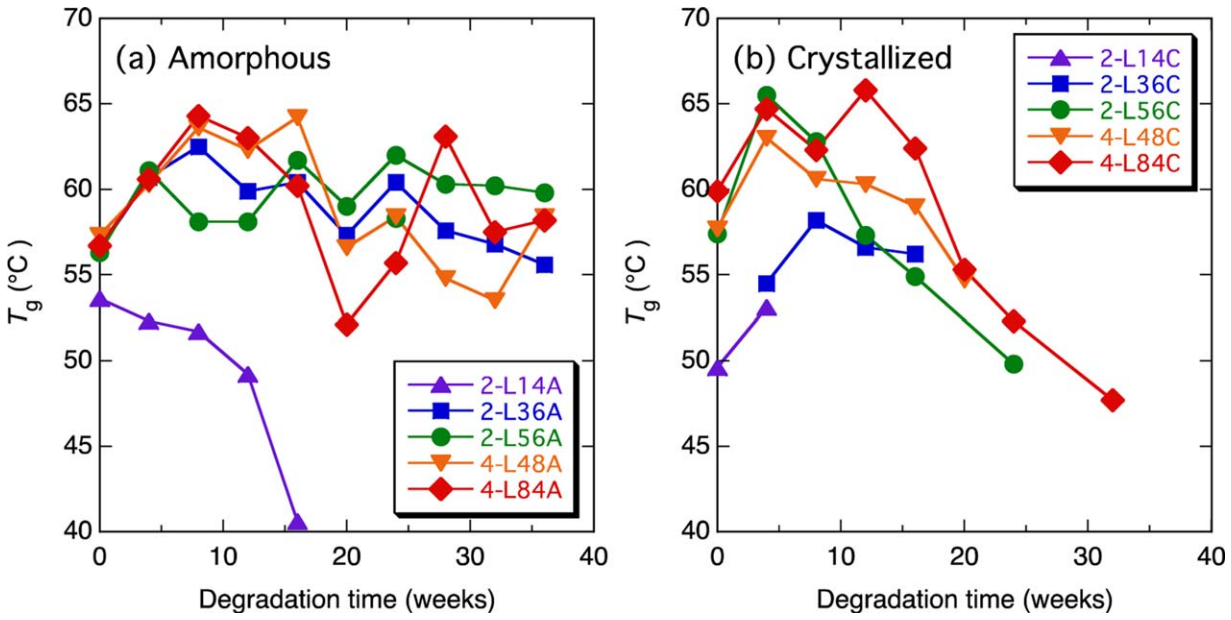

Figure 8. Glass transition temperature (T_g) of initially amorphous (a) and crystallized (b) 2-L and 4-L samples during hydrolytic degradation as a function of degradation time. [Color figure can be viewed in the online issue, which is available at wileyonlinelibrary.com.]

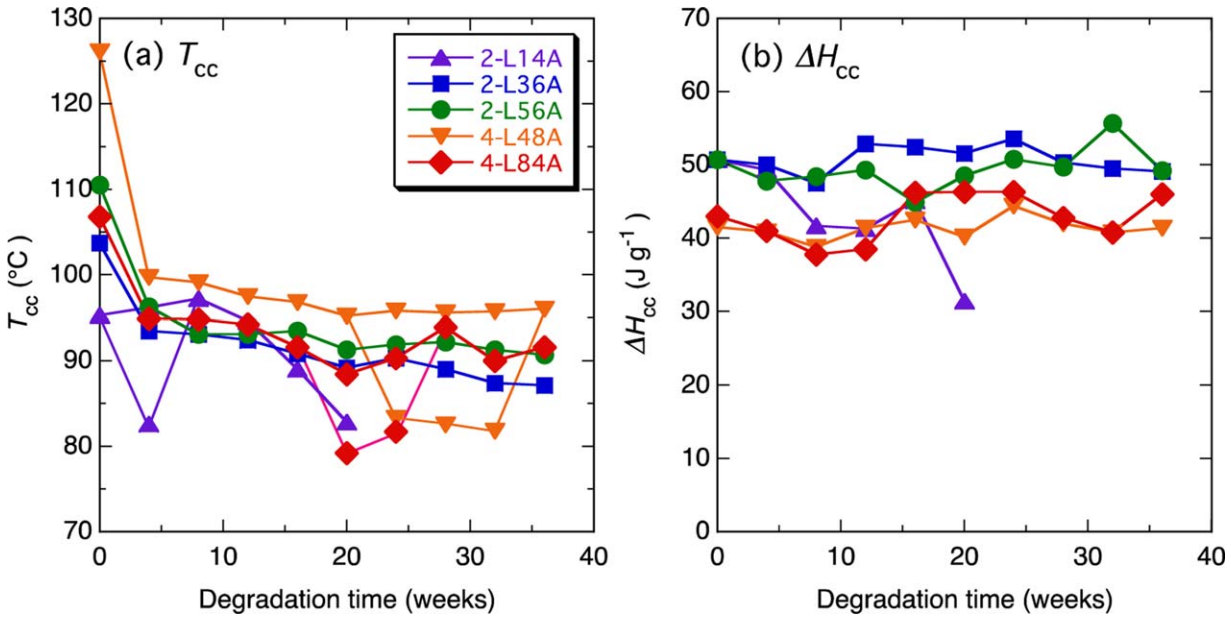

Figure 9. (a) Cold crystallization temperature (T_{cc}) and (b) enthalpy (ΔH_{cc}) of initially amorphous 2-L and 4-L samples during hydrolytic degradation as a function of degradation time. [Color figure can be viewed in the online issue, which is available at wileyonlinelibrary.com.]

respectively. The two T_{cc} values became equivalent at 36 and 28 weeks, respectively, and then the T_{cc} of 4-L84A remained steady for the period of 28–36 weeks. The two T_{cc} values observed for 2-L14A, 4-L48A, and 4-L84A were ascribed to separate crystallization in the domains with high and low chain mobility (because of low and high density chain packing, respectively) or primary and secondary crystallization in one type of domain. To elucidate the reason for the multiple cold crystallization peaks, further detailed study is required. In contrast, the ΔH_{cc} values remained unchanged for the hydrolytic degradation period studied here, except for a gradual decrease in the ΔH_{cc} of 2-L14A, which was caused by a large decrease in molecular weight.

When a double melting peak was observed, the melting subpeak at a lower temperature was regarded as the real melting point of the original crystalline regions, whereas the main melting peak at a higher temperature was due to melting of the crystallites that formed or recrystallized during the DSC heating scan. However, in the present study, since only four and three of the initially amorphous and crystallized samples had low temperature melting subpeaks (Figure 10), respectively, we could not compare the T_m values of the subpeaks for all samples with respect to the original crystalline regions. The T_m of the subpeak (Figure 10) remained steady or slightly increased. The increase in the T_m of the subpeak of 2-L56C was attributed to thickening

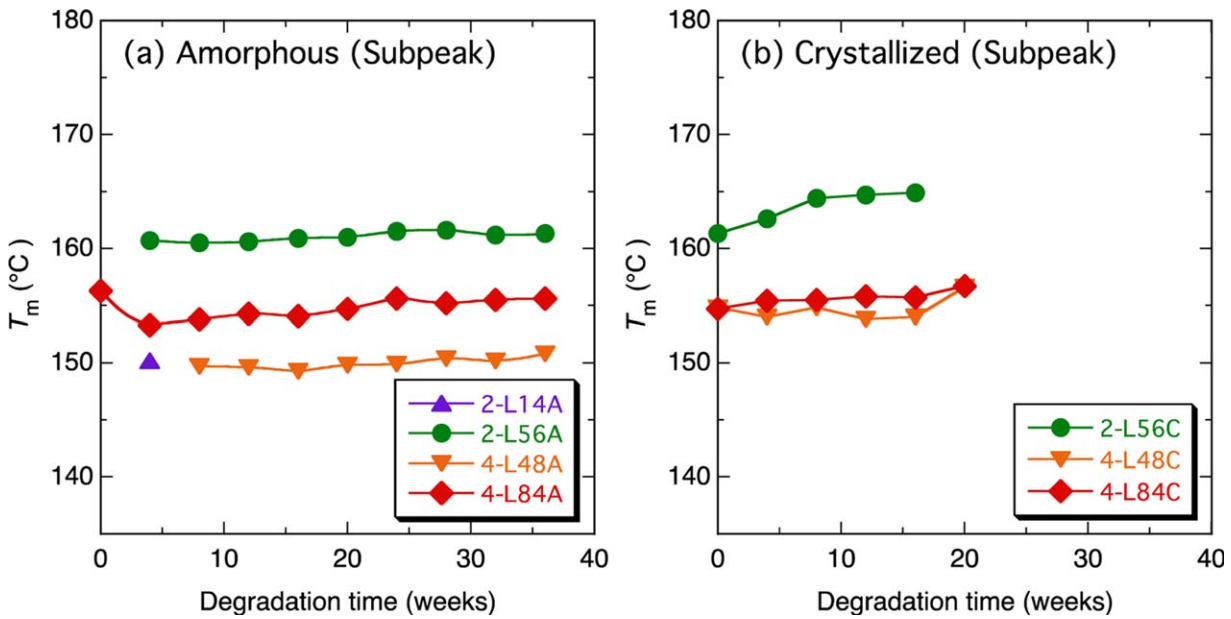

Figure 10. Melting temperature (T_m) of the melting subpeak of initially amorphous (a) and crystallized (b) 2-L and 4-L samples during hydrolytic degradation as a function of degradation time. [Color figure can be viewed in the online issue, which is available at wileyonlinelibrary.com.]

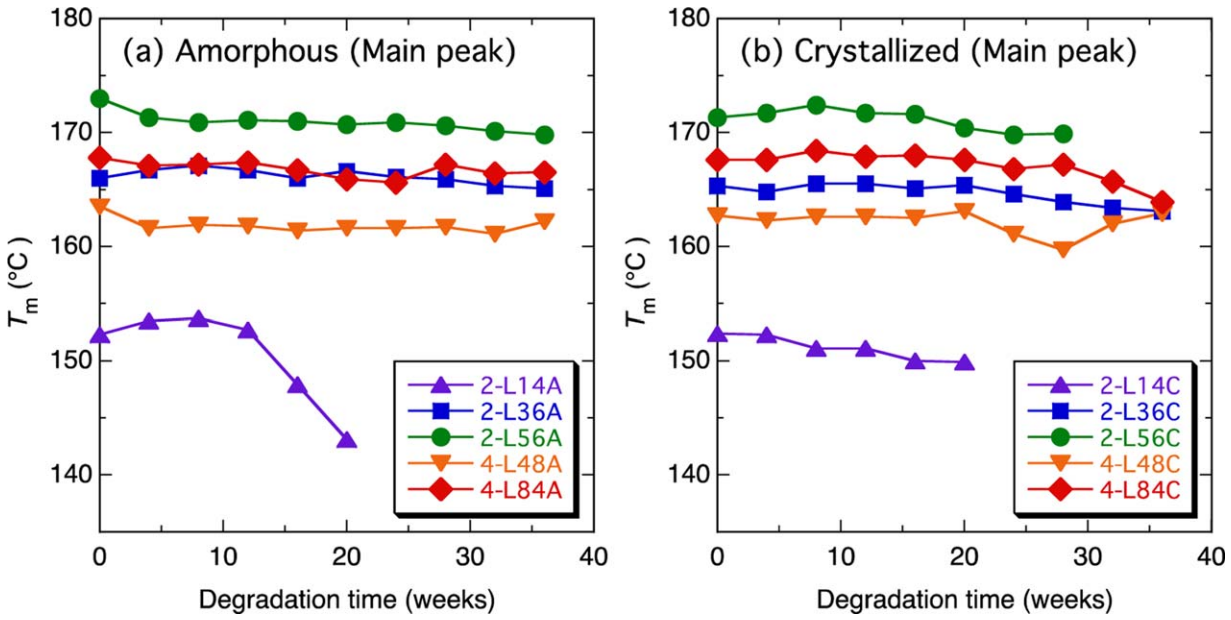

Figure 11. Melting temperature (T_m) of the main melting peak of initially amorphous (a) and crystallized (b) 2-L and 4-L samples during hydrolytic degradation as a function of degradation time. [Color figure can be viewed in the online issue, which is available at wileyonlinelibrary.com.]

of the crystalline regions during hydrolytic degradation; this could have occurred via cleavage of the chains which hindered further crystallization. A very small or no significant decrease in the T_m of the main melting peak was observed for all samples, excluding the rapid decrease of the T_m of 2-L14A in the period exceeding 12 weeks (Figure 11). The rapid decrease in the T_m of the main peak of initially amorphous 2-L14A for the period exceeding 12 weeks, which suggested a large decrease in the crystalline thickness formed during the DSC heating scan, was attributed to the dramatic decrease in molecular weight (Figure 4). On the other hand, a very small or no significant decrease in T_m of other samples was ascribed to the fact that the degradation occurred in the initial stage wherein degradation occurs only in the amorphous region and the crystalline region does not degrade. The decreases in the molecular weights of the samples other than 2-L14A were not sufficient to significantly reduce the T_m.

CONCLUSIONS

The effects of the branching architecture (and/or a high number of hydroxyl groups per unit mass) and crystallinity on hydrolytic degradation and crystallization behavior were investigated using "linear" 2-armed 2-L polymers and "star-shaped" 4-armed 4-L polymers. The degradation mechanism of initially amorphous and crystallized 2-L samples changed from bulk degradation to surface degradation with decreasing initial M_n; in contrast, the degradation mechanism of initially crystallized higher molecular weight 4-L sample was bulk degradation while that of other 4-L samples could not be determined because of the insignificant molecular weight decrease. The hydrolytic degradation rates monitored by molecular weight decrease decreased significantly with greater branching architecture and/or a high number of hydroxyl groups per unit mass. The hydrolytic-degradation rate traced by the decrease in molecular weight was higher for the initially crystallized samples than for the initially amorphous samples; however, the reverse trend was evident for 2-L samples when monitored by weight loss. Initially amorphous 2-L samples with a M_n(GPC) below 3.5×10^4 g mol^{-1} crystallized during hydrolytic degradation. In contrast, a branching architecture and/or high number of hydroxyl groups per unit mass disturbed crystallization of initially amorphous 4-L samples during hydrolytic degradation. All initially crystallized 2-L and 4-L samples had δ-form crystallites before and after hydrolytic degradation. During hydrolytic degradation, the T_g values of initially amorphous and crystallized 2-L and 4-L samples and the T_{cc} values of initially amorphous 2-L and 4-L samples showed changes similar to those reported for 1-armed PLLA.

ACKNOWLEDGMENTS

This research was partly supported by The 21st Century COE Program, "Ecological Engineering for Homeostatic Human Activities," from the Ministry of Education, Culture, Sports, Science and Technology (Japan).

REFERENCES

1. Kharas, G. B.; Sanchez-Riera, F.; Severson, D. K. In Plastics from Microbes; Mobley, D. P., Ed.; Hanser: New York, **1994**; Chapter 4, pp 93–137.
2. Vert, M.; Schwarch, G.; Coudane, J. *J. Macromol. Sci. Pure.: Appl. Chem.* **1995**, *A32*, 787.
3. Hartmann, M. H. In Biopolymers from Renewable Resources; Kaplan, D. L., Ed.; Springer: Berlin, **1998**; Chapter 15, pp 367–411.
4. Garlotta, D. *J. Polym. Environ.* **2001**, *9*, 63.
5. Södergård, A.; Stolt, M. *Prog. Polym. Sci.* **2002**, *27*, 1123.

6. Vert, M. In Encyclopedia of Biomaterials and Biomedical Engineering, Vol. *2*; Wnek, G. E.; Bowlin, G. L. Eds.; Marcel Dekker: New York, **2004**, pp 1254–1263.
7. Auras, R.; Lim, L.-T.; Selke, S. E. M.; Tsuji, H., Eds. Synthesis, Structures, Properties, Processing, and Applications Wiley Series on Polymer Engineering and Technology; Wiley: NJ, **2010**.
8. Slager, J.; Domb, A. J. *Adv. Drug Deliv. Rev.* **2003**, *55*, 549.
9. Tsuji, H. *Macromol. Biosci.* **2005**, *5*, 569.
10. Fukushima, K.; Kimura, Y. *Polym. Int.* **2006**, *55*, 626.
11. Tsuji, H.; Ikada, Y. In Biodegradable Polymer Blends and Composites from Renewable Resources; Yu, L., Ed.; Wiley: New Jersey, **2009**; Chapter 7, pp 165–190.
12. Tsuji, H. In Biodegradable Polymers for Skeletal Implants; Wuisman, P. I. J. M.; Smit, T. H. Eds.; Nova Science Publishers: New York, **2009**; Chapter 3, pp 41–71.
13. Tsuji, H. In Poly(lactic acid): Synthesis, Structures, Properties, Processing, and Applications Auras, R.; Lim, L. -T.; Selke, S. E. M.; Tsuji, H., Eds.; Wiley Series on Polymer Engineering and Technology; Wiley: New Jersey, **2010**, Chapter 21, pp 345–381.
14. Tsuji, H.; Sugiura, Y.; Sakamoto, Y.; Bouapao, L.; Itsuno, S. *Polymer* **2008**, *49*, 1385.
15. Tsuji, H.; Yamamoto, J. *Polym. Degrad. Stab.* **2011**, *96*, 2229.
16. Tsuji, H.; Hayashi, T. *Polym. Degrad. Stab.* **2014**, *102*, 59.
17. Yuan, W.; Zhu, L.; Huang, X.; Zheng, S.; Tang, X. *Polym. Degrad. Stab.* **2005**, *87*, 503.
18. Fu, C.; Zhang, B.; Ruan, C.; Hu, C.; Fu, Y.; Wang, Y. *Polym. Degrad. Stab.* **2010**, *95*, 485.
19. Tsuji, H.; Mizuno, A.; Ikada, Y. *J. Appl. Polym. Sci.* **2000**, *77*, 1452.
20. Andersson, S. R.; Hakkarainen, M.; Inkinen, S.; Södergård, A.; Albertsson, A.-C. *Biomacromolecules* **2012**, *13*, 1212.
21. Sakamoto, Y.; Tsuji, H. *Polymer* **2013**, *54*, 2422.
22. Kim, S. H.; Kim, Y. H. In Biodegradable Plastics and Polymers; Doi, Y.; Fukuda, K., Eds.; Studies in Polymer Science 12, Elsevier: Amsterdam (The Netehrlands), **1993**, pp 464–469.
23. Sakamoto, Y.; Tsuji, H. *Macromol. Chem. Phys.* **2013**, *214*, 776.
24. Schwach, G.; Vert, M. *Int. J. Biol. Macromol.* **1999**, *25*, 283.
25. Tsuji, H.; Ikada, Y. *Polymer* **1995**, *36*, 2709.
26. de Jong, S. J.; Arias, E. R.; Rijkers, D. T. S.; van Nostrum, C. F.; Kettenes-van den Bosch, J. J. *Polymer* **2001**, *42*, 2795.
27. Zhang, J.; Tashiro, K.; Tsuji, H.; Domb, A. J. *Macromolecules* **2007**, *40*, 1049.
28. Kawai, T.; Rahma, N.; Matsuba, G.; Nishida, K.; Kanaya, T.; Nakano, M.; Okamoto, H.; Kawada, J.; Usuki, A.; Honma, N.; Nakajima, K.; Matsuda, M. *Macromolecules* **2007**, *40*, 9463.
29. Pan, P.; Zhu, B.; Kai, W.; Dong, T.; Inoue, Y. *J. Appl. Polym. Sci.* **2008**, *107*, 54.
30. Bouapao, L.; Tsuji, H.; Tashiro, K.; Zhang, J.; Hanesaka, H. *Polymer* **2009**, *50*, 4007.
31. Wasanasuk, K.; Tashiro, K. *Polymer* **2011**, *52*, 6097.
32. Li, S.; Garreau, H.; Vert, M. *J. Mater. Sci.: Mater. Med.* **1990**, *1*, 198.
33. Leenslag, J. W.; Pennings, A. J.; Bos, R. R. M.; Rozema, F. R.; Boering, G. *Polymer* **1987**, *8*, 311.
34. Matsusue, Y.; Yamamuro, T.; Oka, M.; Shikinami, Y.; Hyon, S. H.; Ikada, Y. *J. Biomed. Mater. Res.* **1992**, *26*, 1553.
35. Duek, E. A. R.; Zavaglia, C. A. C.; Belangero, W. D. *Polymer* **1999**, *40*, 6465.
36. Tsuji, H.; Ikada, Y. *Polym. Degrad. Stab.* **2000**, *67*, 179.